

MUTLISCALE SURROGATE MODELING AND UNCERTAINTY QUANTIFICATION FOR PERIODIC COMPOSITE STRUCTURES

Charilaos Mylonas¹, Bemetz Valentin¹, Eleni Chatzi¹

¹ Department of Civil, Environmental
and Geomatic Engineering,
ETH Zürich
Stefano-Franscini-Platz 5, 8093 Zürich
e-mail: mylonasc@ibk.baug.ethz.ch

Keywords: Polynomial Chaos Expansions, Asymptotic Expansion Homogenization, Composite Analysis, Principal Component Analysis, Random Microstructure

Abstract. *Computational modeling of the structural behavior of continuous fiber composite materials often takes into account the periodicity of the underlying micro-structure. A well established method dealing with the structural behavior of periodic micro-structures is the so-called Asymptotic Expansion Homogenization (AEH). By considering a periodic perturbation of the material displacement, scale bridging functions, also referred to as elastic correctors, can be derived in order to connect the strains at the level of the macro-structure with micro-structural strains. For complicated inhomogeneous micro-structures, the derivation of such functions is usually performed by the numerical solution of a PDE problem - typically with the Finite Element Method. Moreover, when dealing with uncertain micro-structural geometry and material parameters, there is considerable uncertainty introduced in the actual stresses experienced by the materials. Due to the high computational cost of computing the elastic correctors, the choice of a pure Monte-Carlo approach for dealing with the inevitable material and geometric uncertainties is clearly computationally intractable. This problem is even more pronounced when the effect of damage in the micro-scale is considered, where re-evaluation of the micro-structural representative volume element is necessary for every occurring damage. The novelty in this paper is that a non-intrusive surrogate modeling approach is employed with the purpose of directly bridging the macro-scale behavior of the structure with the material behavior in the micro-scale, therefore reducing the number of costly evaluations of corrector functions, allowing for future developments on the incorporation of fatigue or static damage in the analysis of composite structural components.*

1 Introduction

Continuous fiber reinforced polymer composites are light, stiff materials of significantly improved static strength and fatigue resistance. For the engineering analysis of such materials, a direct discretization of the fine spatial variation of the composite material would render the problem computationally intractable. Therefore, composite engineering analysis seeks to deliver a consistent calculation of the effective macroscopic properties by considering the material and geometrical properties of the micro-structure (*homogenization*) and adequately approximating the stresses in the micro-structure (*localization*¹). A mathematically rigorous approach to the problem of homogenization and localization, that further applies to the problem of elasticity in the context of composite materials, was proposed in [1].

The aforementioned technique is often termed *Asymptotic Expansion Homogenization* (AEH). The application of the method relies on the assumption that displacement appears into well separated spatial scales. The method yields effective elastic properties on the macro-scale without any assumptions on the distribution of strains or stresses in the micro-scale, but only with the assumption of periodicity in the displacements among different representative volume elements. For a more detailed, engineering oriented derivation of the AEH method for elasticity the reader is referred to [2] and [3]. Extending the AEH method to damaged composites has also attracted research interest [4, 5]. In the context of another homogenization framework, it has been shown that efficient hysteretic multi-scale damage models can be derived [6].

The complete determination of material properties and microstructure geometry is, in general, not possible. Therefore, the prediction of the material response in the micro-scale should account for uncertainty. A direct Monte-Carlo approach for the purpose of representing the effect of all the uncertain parameters would quickly become intractable.

In the present work we investigate the potential of non-intrusive probabilistic uncertainty propagation techniques, namely the Polynomial Chaos Expansion (PCE)[7], for the purpose of constructing surrogate models. Efficient surrogate modelling techniques are expected to yield further reductions in the computational cost of multi-scale finite element analysis. An intrusive PCE for the same problem was proposed in [8].

Finally, a dimensionality reduction technique, namely Principal Component Analysis (PCA) was found to be highly efficient on decomposing the stiffness tensor without strong assumptions on the geometry induced symmetries of the homogenized stiffness tensor.

The uncertainty quantification toolbox UQLab was used for deriving the PCE of the homogenized stiffness tensor [9].

2 Computational Methodology

In the following the basic components of the Asymptotic Expansion Homogenization for analyzing elastic periodic structures and the Polynomial Chaos Expansion surrogate modelling technique, used in the present study are going to be briefly presented.

2.1 Asymptotic Expansion Homogenization

This section serves for establishing notation and introducing an intuitive understanding of the quantities related to the problem of homogenization and localization for periodic media. We denote $\mathbf{x} = \{x_1, x_2, x_3\}$ as the coordinate system of a composite structure, and further introduce a coordinate system local to every representative volume element (microstruc-

¹Not to be confused with *localization* in the context of damage detection. Some authors use the term *de-homogenization* to avoid confusion.

ture) $\mathbf{y} = \{y_1, y_2, y_3\}$. Quantities marked with \cdot^ϵ denote the high resolution quantities in the macro-scale. All indices attain values in $\{1, 2, 3\}$. Einstein summation is implied for repeating indices. We seek to solve the elasticity boundary value problem,

$$\frac{\partial \sigma_{ij}^\epsilon}{\partial x_j^\epsilon} + f_i = 0 \quad \text{in } \Omega \quad (1)$$

$$u_i^\epsilon = 0 \quad \text{on } \partial_1 \Omega \quad (2)$$

$$\sigma_{ij}^\epsilon n_j = F_i \quad \text{on } \partial_2 \Omega \quad (3)$$

$$\epsilon_{ij}(\mathbf{u}^\epsilon) = \frac{1}{2} \left(\frac{\partial u_i^\epsilon}{\partial x_j^\epsilon} + \frac{\partial u_j^\epsilon}{\partial x_i^\epsilon} \right) \quad (4)$$

$$(5)$$

where $\partial_1 \Omega$ and $\partial_2 \Omega$ denote different boundaries, $u_i^\epsilon = \mathbf{u}^\epsilon(\mathbf{x})$ is the displacement of the macro-structure, F_i a traction force, and f_i the body force. The constitutive relation simply reads

$$\sigma_{ij}^\epsilon = D_{ijkl}^\epsilon \epsilon_{kl}. \quad (6)$$

Due to the geometry of the continuous fiber reinforced composites, D_{ijkl}^ϵ is varying periodically in the material, in a scale much finer than the scale of the structure. It is convenient to define the so-called *scale* parameter $\epsilon \ll 1$, which represents the ratio between the microscopic and macroscopic scale. Considering the coordinates of the micro-scale and the macroscale, one may write $y_i = x_i/\epsilon$. By the chain rule we have

$$\frac{\partial \cdot}{\partial x_i^\epsilon} = \frac{\partial \cdot}{\partial x_i} + \frac{1}{\epsilon} \frac{\partial \cdot}{\partial y_i} \quad (7)$$

The displacements are represented with the following expansion in, ϵ , as

$$\mathbf{u}_i^\epsilon(\mathbf{x}) = \mathbf{u}^{(0)}(\mathbf{x}) + \epsilon \mathbf{u}^{(1)}(\mathbf{x}) + \epsilon^2 \mathbf{u}^{(2)}(\mathbf{x}) + \dots \quad (8)$$

It has been rigorously established [1], that by plugging Equation 8 into the problem of elasticity, and by passing to the limit $\epsilon \rightarrow 0$, the elasticity problem boils down to a hierarchical set of partial differential equations. It is assumed that the displacements in the representative volume elements are connected to the gradients of the displacement in the macro-scale $\frac{\partial u_k^{(0)}}{\partial x_l}(\mathbf{x})$ by a certain vector valued function $\chi_i^{kl}(\mathbf{y})$. This approximation reads

$$u_i^{(1)}(\mathbf{x}, \mathbf{y}) = -\chi_i^{kl}(\mathbf{y}) \frac{\partial u_k^{(0)}}{\partial x_l}(\mathbf{x}) + \bar{u}_i^{(1)}(\mathbf{x}), \quad (9)$$

where $\bar{u}_i^{(1)}(\mathbf{x})$ denotes the average displacement of the representative unit cell in the macro-scale coordinate system. Function χ_i^{mn} is often termed the *elastic corrector*. Note that every pair of components mn correspond to a different spatial gradient. The accuracy of this approximation relies on the existence of the gradients $\frac{\partial u_k^{(0)}}{\partial x_l}(\mathbf{x})$ and assumes a slow variation in the macroscopic scale.

For continuous fiber composites, without stress concentrations this is a reasonable assumption. A stress concentration may be due to localized damage, i.e., due to a macroscopic crack or very close to the boundaries of the composite structure².

²On the other hand, the effect of diffuse slowly spatially varying damage may be well approximated without the presented framework to break down.

For a first order (first order perturbation) approximation of the perturbed displacement field, assuming χ_i^{mn} smooth in Ω and smooth and periodic with zero mean in the RVE or $\in \mathcal{V}^{per}$ on Ω_Y , the variational problem

$$\int_{\Omega_Y} D_{ijkl} \frac{\partial \chi_k^{mn}}{\partial y_l} \frac{\partial \nu_i}{\partial y_j} d\mathbf{y} = \int_{\Omega_Y} D_{ijmn} \frac{\partial \nu_j}{\partial y_i} d\mathbf{y} \quad (10)$$

holds. We seek solutions for χ_i^{mn} so that Equation 10 holds for all $\nu_i \in \mathcal{V}^{per}$.

Due to the symmetries of the stiffness tensor, we have $D_{ijmn} = D_{ijnm} = D_{jimn}$. Therefore, we only need to consider $mn = \{11, 22, 33, 23, 13, 12\}$ for the full computation of the elastic corrector. In practice Equation 10 results in 6 variational problems for the computation of the corrector, one for every different value of mn .

The variational problem allows for a finite element approximation of the corrector function. By considering the RVE averaged strains and stresses, an approximation of the stiffness tensor $D_{ijkl}^\epsilon \approx D_{ijkl}^h$ in the macro-scale is possible. Namely,

$$D_{ijkl}^h = \frac{1}{|Y|} \int_{\Omega_Y} D_{ijkl}(\mathbf{y}) \left[\delta_{kl} \delta_{ln} - \frac{\partial \chi_k^{mn}}{\partial y_l} \right] d\mathbf{y} \quad (11)$$

In practice, even for the case of homogeneous materials described by Lamé parameters in the micro-scale, the homogenized stiffness tensor turns out anisotropic. Some symmetries may be induced by the geometry, such as orthotropy and transverse isotropy, but the framework presented in the present work is concerned with the case of the fully anisotropic material.

It is apparent that since the corrector connects the displacements of the macro-structure to the displacements of the micro-structure, strains and stresses can be straight-forwardly computed for the micro-structure. Namely the micro-stresses are computed with

$$\sigma_{ij}^{(1)}(\mathbf{x}) = D_{ijkl} \left(\delta_{mk} \delta_{nl} - \frac{\partial \chi_k^{mn}}{\partial y_l} \right) \frac{\partial u^{(0)}}{\partial x_n}. \quad (12)$$

Therefore by storing the solution of the corrector we may directly compute stresses in the micro-scale without making any strong assumptions on the distribution of stresses or strains on the boundaries of the RVE. The only assumption required for this framework is the periodicity of displacements in the boundaries of the RVE.

For the actual solution of the finite element discretization of Equation 10, periodic boundary conditions have to be enforced. In addition, one arbitrary point must be constrained to zero in all components of χ_i^{mn} since the weak form has a unique solution up to an additive constant. Due to the periodicity of the corrector, and the fact that homogenization and localization problems are concerned only with derivatives of the corrector, the boundary conditions are essentially equivalent to the zero-mean requirement for the corrector function.

2.2 Polynomial Chaos Expansions

Polynomial chaos expansions (PCE) were first introduced in [10] for Gaussian input variables and generalized in [7] for classical probability distribution functions. Consider a set of random inputs $\mathbf{X} = \{x_1, x_2, \dots, x_n\}$ to a deterministic model $Y = \mathcal{M}(\mathbf{X})$. The method relies in the construction of a tensor product basis of univariate polynomials $\Phi^{(n)}(x_n)$, orthogonal with respect to inner products weighted by probability distribution functions $f_X(x_n)$. The orthogonality relation reads,

$$\langle \Phi_i^{(m)}, \Phi_j^{(m)} \rangle_{f_X} = \delta_{ij} \quad (13)$$

where

$$\langle f, g \rangle_{f_X} = \int f(x)g(x)f_X(x)dx \quad (14)$$

and δ_{ij} is the Kroneker delta. The tensor product basis set reads,

$$\Psi(\mathbf{X}) = \otimes_{m=1}^n \Phi^{(m)} \quad (15)$$

where $\Phi^{(m)} = \{\Phi_1^{(m)}, \Phi_2^{(m)}, \dots\}$ with superscript denoting the input dimension and subscript denoting the order of the orthogonal polynomial.

A PCE model, is a linear combination of the elements of Equation 15,

$$\mathcal{M}(\mathbf{X}) = \sum_{\mathbf{a} \in \mathcal{A}} c_{\mathbf{a}} \Psi_{\mathbf{a}}(\mathbf{X}) \quad (16)$$

indexed by $\mathbf{a} = \{a_1, a_2, \dots, a_m\}$, which is a multi-index that denotes the degree of the univariate polynomials of each of the input variables, and \mathcal{A} the set of multi-indices. For example,

$$\Psi_{\mathbf{a}} = \Phi_{a_1}^{(1)}(x_1) \Psi_{a_2}^{(2)}(x_2) \dots \Psi_{a_n}^{(n)}(x_n) \quad (17)$$

where a_i denotes the degree of orthogonal polynomials along dimension i . In the presented case the number of random input dimensions is $n = 6$. In practice, the set of multi-indices, is truncated for numerical implementation. Also the PCE is considered up to a certain degree of univariate polynomials in each dimension to render the problem numerically tractable. According to the Cameron-Martin theorem [11, 7], such an expansion converges in the L_2 sense, when $\mathcal{M}(\mathbf{X})$ has finite variance.

There are several approaches for the purpose of determining the coefficients $c_{\mathbf{a}}$. The most versatile method, that also deals automatically with adaptively selecting basis elements, is the Least Angle Regression (LAR)[12] approach. LAR is the method of choice for the present work. See [13] and [14] for a discussion of the benefits of LAR.

3 Example application on continuous fibre reinforced composites

A typical composite structure, composed of transversely isotropic glass fibers embedded in a polymer matrix with stacking sequence $[0, -\phi, +\phi]$, was analyzed as a proof of concept. The material properties adopted herein, are given in Table 1. In this study, only geometric variation of the micro-structure was considered. For the purpose of demonstrating the effectiveness of the PCE surrogate model of the homogenization process, relatively large variations on the geometrical parameters of the micro-structure were chosen. The ranges of the parameters chosen for the present work are given in Table 2.

V_{f_1} corresponds to the volume fraction of the 0° fibers and V_{f_2} the volume fraction of each of the layers of the $\pm 45^\circ$ fibers. Correspondingly, a_1, a_2 are the major radii of the elliptical cross section of the fibers and b_1, b_2 the minor radii (Figure 1). A uniform distribution is considered for the aforementioned parameters, in the ranges presented in Table 2. In the current study, 200 model runs were used, with input vectors randomly sampled with Latin Hypercube Sampling (LHS) in order to explore the parameter space as well as possible with the limited budget of model runs. A visual account of the solution for the corrector function for a particular set of parameters is given in Figure 2.

| | Fiber | Matrix |
|-------------|-------|--------|
| E_1 [GPa] | 31 | 2.79 |
| E_2 [GPa] | 7.59 | 2.76 |
| ν | 0.3 | 0.3 |
| G_{12} | 3.52 | 1.1 |
| G_{23} | 2.69 | 1.1 |

Table 1: Material properties of the micro-structure.

| Parameter | min | max |
|-------------------------|-------|-------|
| V_{f_2} | 0.600 | 0.74 |
| $V_{f_1} \cdot V_{f_2}$ | 0.600 | 1.00 |
| a_2 | 0.450 | 0.55 |
| $a_1 \cdot b_1$ | 0.167 | 0.250 |
| $a_2 \cdot b_2$ | 0.167 | 0.250 |
| ϕ | 15 | 75 |

Table 2: Assumed micro-structure geometry parameter variations.

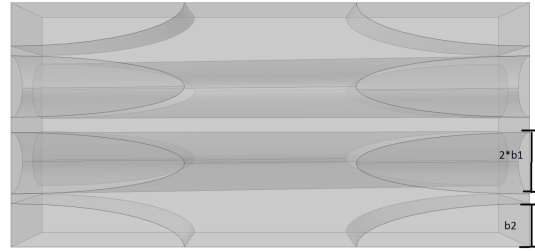
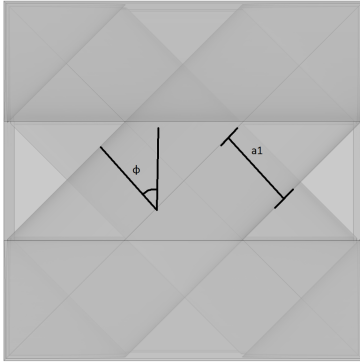


Figure 1: Random geometric parameters of the micro-structure. The volume fractions affect the intra-fiber spacing.

3.1 Dimensionality reduction with PCA for the homogenized stiffness tensor

It is natural to expect that the components of the homogenized stiffness tensor co-vary. In general, for arbitrary micro-structure geometries it is not trivial to assess intuitively the effect of geometric variation on the stiffness tensor directly. In the present study, Principal Component Analysis (PCA) is implemented for the reduction of the 6×6 homogenized random stiffness tensor. In order to apply PCA on the homogenized tensors, the components of every random tensor are first flattened to a row vector as indicated in Equation 18.

A set of N^{PCA} principal components $D_{PCA}^{(m)}$ (corresponding to tensor components) is sought, that satisfy Equation 19, where μ_{D^h} is the empirical mean of the homogenized stiffness, \mathbf{X}_n is the n^{th} realization of the random input vector and $\lambda^{(m)}(\mathbf{X}_n)$ denotes a random coefficient that depends on the n^{th} realization of the random input data.

$$D_{ijkl}^h(\mathbf{X}_i) = \begin{bmatrix} D_{1111} & D_{1122} & D_{1133} & 0 & 0 & 0 \\ & D_{2222} & D_{2233} & 0 & 0 & 0 \\ & & D_{3333} & 0 & 0 & 0 \\ & & & D_{2323} & 0 & 0 \\ & Sym & & & D_{1313} & 0 \\ & & & & & D_{1212} \end{bmatrix} \rightarrow \left\{ \begin{matrix} D_{1111} \\ D_{2222} \\ D_{3333} \\ D_{2323} \\ D_{1313} \\ D_{1212} \\ D_{2233} \\ D_{1133} \\ D_{1122} \end{matrix} \right\}^T \quad (18)$$

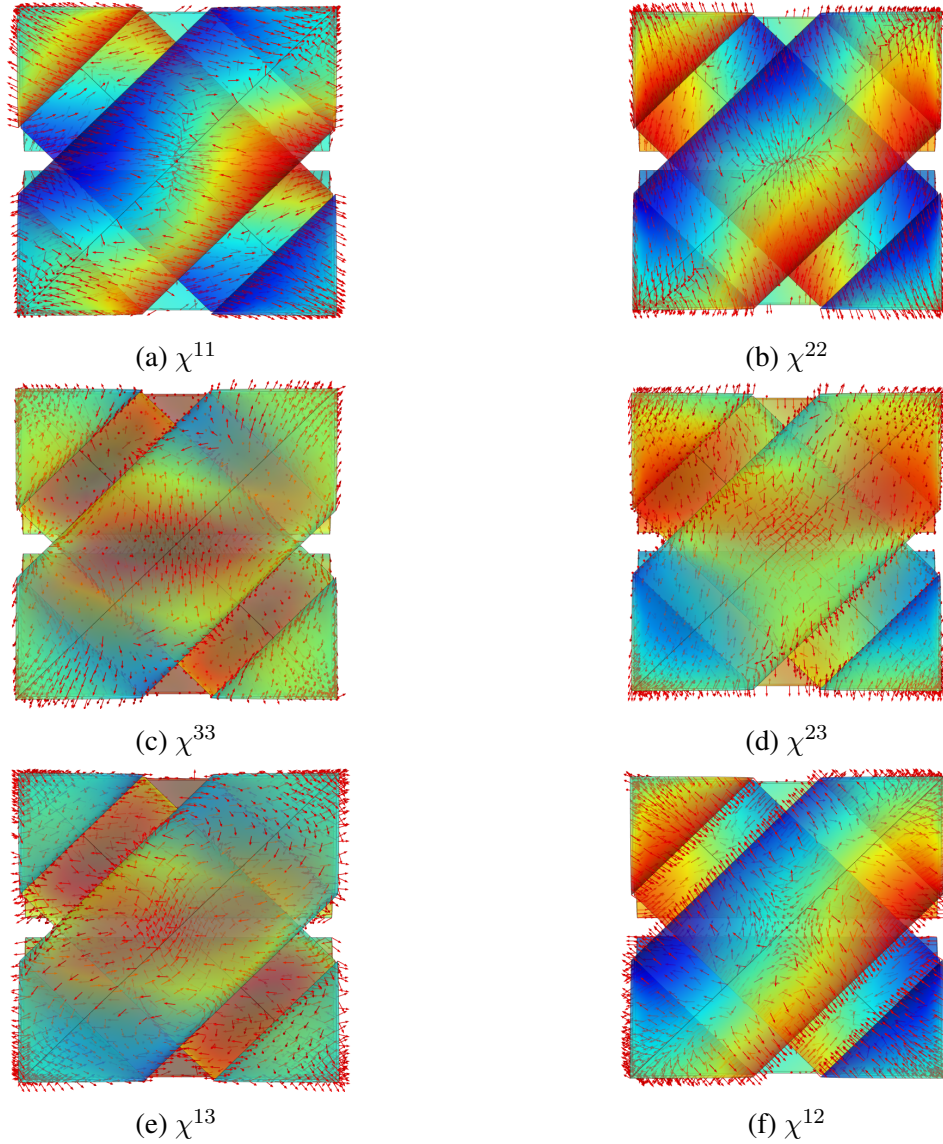


Figure 2: A visual account of the corrector function for a composite with $\phi = 45^\circ$. The correctors are plotted only on the surface of the fibers and the top layer of 0° fibers are hidden. The color corresponds to $(\chi_1^{mn})^2 + (\chi_2^{mn})^2 + (\chi_3^{mn})^2$. Although not easily visible due to 3D plotting, the solution for the corrector is periodic.

$$D_{ijkl}^h(\mathbf{X}_n) = \sum_{m=1}^{N^{PCA}} \lambda^{(m)}(\mathbf{X}_n) \cdot D_{PCA}^{(m)} + \mu_{D^h} \quad (19)$$

For the present study, the tensor is symmetric and it is expected to correspond to an orthotropic elastic material. This results in 9 non-zero components. For a general anisotropic elastic material, up to 21 components would be expected. Polynomial surrogates and sensitivity analysis for generally anisotropic materials described by probabilistically modelled random materials and random geometry may be treated via the same framework in a straightforward manner without placing any assumptions on the form of the stiffness tensor. The 4 first principal components were employed herein. Their contributions to the variance of the data are summarized in table Table 3. Considering the variance explained, it is concluded that 4 components are sufficient

to capture the main variations on the homogenization data. The variance due to the remaining 5 principal components is considered insignificant, and attributed to the slight inaccuracies of the FE solution. For illustrative purposes, the two first principal components are presented in Table 4.

| Component | $D_{PCA}^{(1)}$ | $D_{PCA}^{(2)}$ | $D_{PCA}^{(3)}$ | $D_{PCA}^{(4)}$ |
|--------------------|-----------------|-----------------|-----------------|-----------------|
| Explained Variance | 50.01% | 35.45% | 14.10% | 0.39 % |

Table 3: Variance explained by the first 4 principal components.

In what follows, polynomial chaos expansions and Sobol’ sensitivity analysis are implemented on the coefficients of the 4 principal components. Polynomial chaos expansion is constructed from a tensor product basis of polynomials orthogonal with respect to the probability distribution of the random inputs of our problem. In the present problem, since the distribution of all input random variables is uniform, a basis composed of multivariate tensor products of *Legendre* polynomials in each of the input variables of Table 2 is employed. Namely, polynomial chaos expansion is sought in the form

$$\hat{D}_{PCE}^h(\mathbf{X}) = \sum_{m=1}^{N^{PCA}} \sum_{\mathbf{a} \in \mathcal{A}} c_{\mathbf{a}}^{(m)} \Psi_{\mathbf{a}}(\mathbf{X}) D_{PCA}^{(m)} \quad (20)$$

with $\mathbf{X} = \{x_1, \dots, x_6\}$ denoting the random parameters of the micro-structure, $D_{PCA}^{(m)}$ and $m = \{1, 2, \dots, N^{PCA}\}$ denoting the principal components. In our case $N^{PCA} = 4$.

The linear PCA approach adopted herein straightforwardly allows for the approximate reconstruction of the original stiffness tensors. The same approach was assessed in the context of health monitoring in [15].

The polynomial chaos expansion is computed by means of Least Angle Regression (LAR) [13]. The quality of the PCE least angle regression fit is measured with the generalized LOO error [16]. In Table 5 various parameters indicative of the quality of the PCE regression fit are summarized, separately for different principal components of the homogenized tensor. A visual account of the quality of the fit for all reconstructed stiffness tensor components, is demonstrated by plotting the reconstructed components against the original simulation data in Figure 3.

The performance of the fit is considered as satisfactory. In the next section the effect of the variability of the input variables to the homogenized stiffness is to be quantified by means of Sobol’ sensitivity indices. A set of histograms for the stiffness matrix component coefficients is given in Figure 4. These histograms were computed by sampling from the polynomial chaos surrogate with 10^4 samples.

3.2 Sobol’ Sensitivity Analysis

As demonstrated in [17] it is possible to efficiently compute the Sobol’ global sensitivity indices through the coefficients of a polynomial chaos surrogate model. Sensitivity analysis is performed separately for each one of the 4 principal components of the PCA. The results are presented in Figure 5. It should be noted that the results of the sensitivity analysis on the $\lambda^{(m)}$ have a meaning that is not decoupled from the values of the principal components $D_{PCA}^{(m)}$ themselves (Table 4). In a setting where the principal components had an interpretable meaning such an analysis would have been more beneficial.

$$D_{PCA}^{(1)} = \begin{bmatrix} 0.60 & 0.11 & 0.05 & 0 & 0 & 0 \\ 0.11 & 0.46 & 0.05 & 0 & 0 & 0 \\ 0.05 & 0.05 & 0.16 & 0 & 0 & 0 \\ 0 & 0 & 0 & 0.25 & 0 & 0 \\ 0 & 0 & 0 & 0 & 0.27 & 0 \\ 0 & 0 & 0 & 0 & 0 & 0.50 \end{bmatrix}$$

$$D_{PCA}^{(2)} = \begin{bmatrix} 0.74 & -0.12 & -0.01 & 0 & 0 & 0 \\ -0.12 & -0.14 & -0.02 & 0 & 0 & 0 \\ -0.01 & -0.02 & -0.04 & 0 & 0 & 0 \\ 0 & 0 & 0 & -0.10 & 0 & 0 \\ 0 & 0 & 0 & 0 & -0.04 & 0 \\ 0 & 0 & 0 & 0 & 0 & -0.64 \end{bmatrix}$$

Table 4: First two principal components of the random homogenized stiffness tensor.

| Component | PCE-LOO Error | Normalized MSE | PCE Maximum Degree |
|-----------------|---------------|----------------|--------------------|
| $\lambda^{(1)}$ | $1.90e-3$ | $1.6e-3$ | 6 |
| $\lambda^{(2)}$ | $2.05e-3$ | $1.7e-3$ | 5 |
| $\lambda^{(3)}$ | $1.81e-3$ | $1.3e-3$ | 5 |
| $\lambda^{(4)}$ | $7.17e-2$ | $5.0e-2$ | 5 |

Table 5: PCE least-squares regression fit quality measures and maximum degree of expansion for the principal components with LAR.

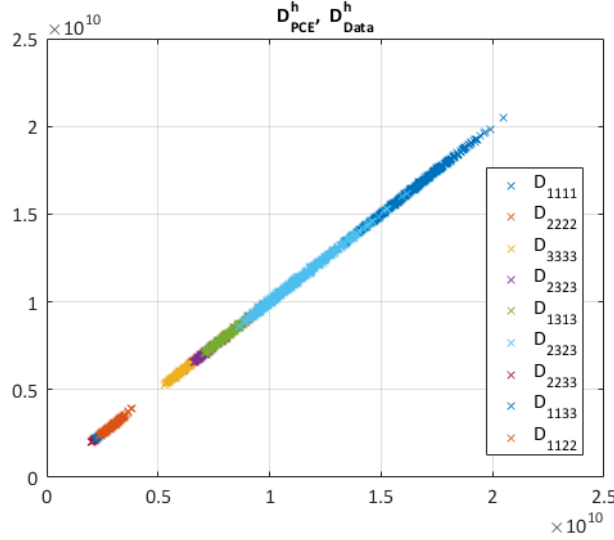


Figure 3: Quality of fit for the stiffness tensor. The tensor components are retrieved by using the PCE approximated PCA component coefficients with the principal component vectors.

Nevertheless, in our setting, it is clear that the angle of the $\pm\phi^\circ$ fibers is a significant factor, along with V_{f_2} and the ratio of the volume fractions of $\pm\phi^\circ$ and 0° fibers. It is interesting to observe, that the shape of the fibers, represented by a_1, a_2, b_1, b_2 has an almost negligible effect on the homogenization problem, at least for the range of variations considered in the present study. The high sensitivity index in the 4th principal component is considered negligible, in light of the small contribution to the variance in the context of PCA of $\lambda^{(4)}$.

3.3 Conclusion

A framework for the construction of efficient and accurate polynomial surrogate models is presented for the problem of homogenization of parametrized, probabilistically modelled random microstructures. A limited budget of random Monte-Carlo runs is employed together with a non-intrusive surrogate modelling approach. Linear Principal Component Analysis was found sufficient for the data-driven dimensionality reduction of the random realizations of the stiffness tensor. Efficient PCE-based global sensitivity analysis was performed, yielding quantitative results on the effect of different random input parameters on the composite macro-scale response.

The utility of PCE models for the homogenization and localization problems is not limited to the gaining of a deeper insight on the effect of uncertainty of input parameters on homogenization through sensitivity analysis, as demonstrated in the present study. Although in the present work homogenization surrogates are exclusively presented, a rather simple extension in the same framework would pertain to the construction of surrogate models for the problem of micro-strain computation under uncertainty. This will form part of future investigations. The efficient solution of the stress localization problem efficiently is an important stepping stone towards the goal of highly efficient multi-scale damage prediction for composites of an arbitrary micro-structure.

Acknowledgement: The authors would like to gratefully acknowledge the support of the European Research Council via the ERC Starting Grant WINDMIL (ERC-2015-StG #679843) on the topic of Smart Monitoring, Inspection and Life-Cycle Assessment of Wind Turbines.

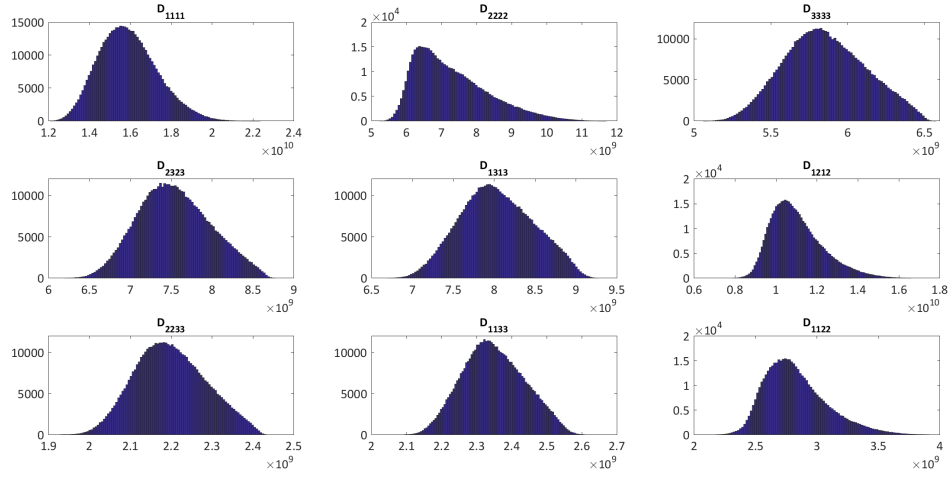


Figure 4: Histogram of coefficients of the homogenized stiffness matrix for the selected variation of parameters.

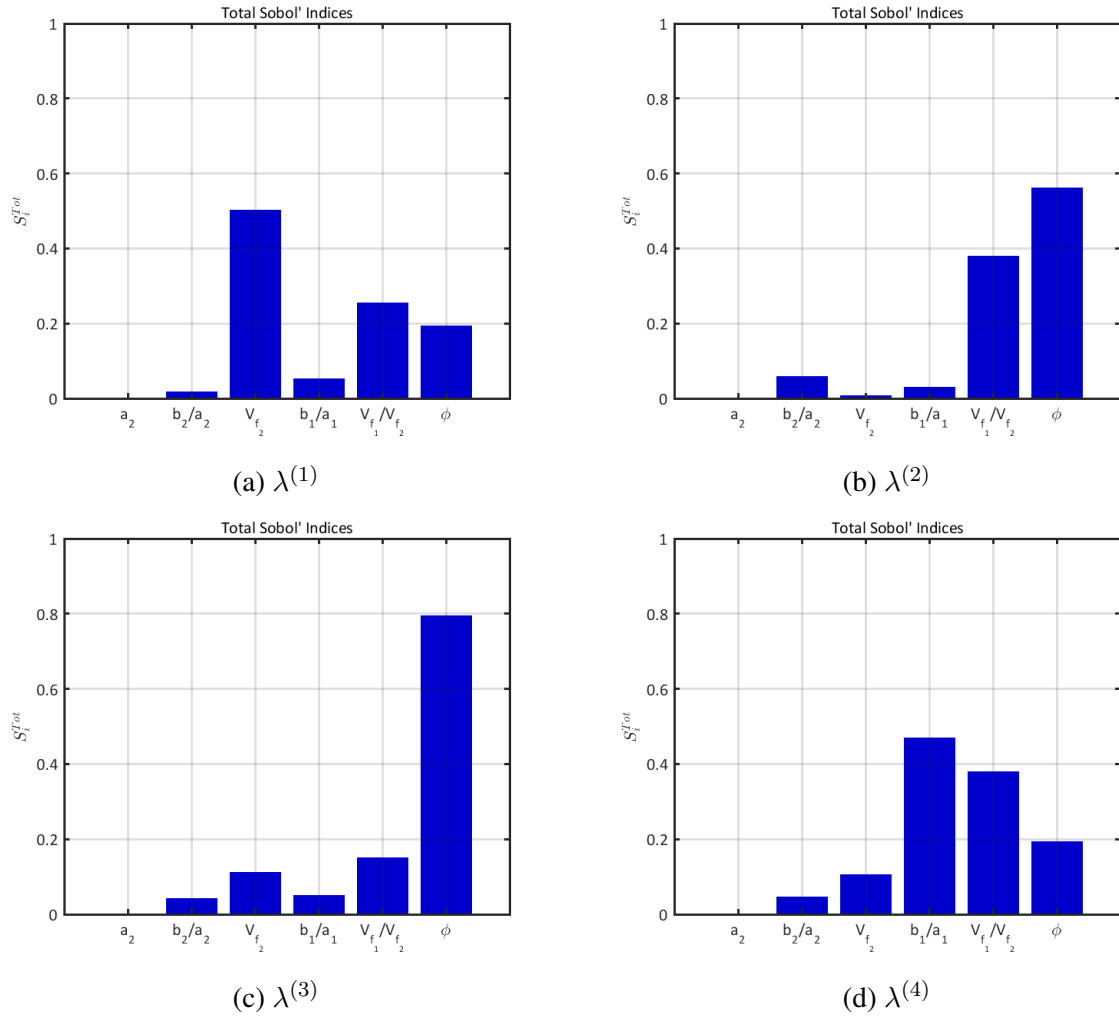


Figure 5: Sobol' sensitivity indices for the different components of the PCA of the homogenized tensor data.

REFERENCES

- [1] Alain Bensoussan, Jacques-Louis Lions, and George Papanicolaou. *Asymptotic analysis for periodic structures*, volume 5. North-Holland Publishing Company Amsterdam, 1978.
- [2] Peter W Chung, Kumar K Tamma, and Raju R Namburu. Asymptotic expansion homogenization for heterogeneous media: computational issues and applications. *Composites Part A: Applied Science and Manufacturing*, 32(9):1291–1301, 2001.
- [3] J. Pinho da Cruz, J.A. Oliveira, and F. Teixeira-Dias. Asymptotic homogenisation in linear elasticity. part i: Mathematical formulation and finite element modelling. *Computational Materials Science*, 45(4):1073 – 1080, 2009.
- [4] Caglar Oskay and Jacob Fish. Eigendeformation-based reduced order homogenization for failure analysis of heterogeneous materials. *Computer Methods in Applied Mechanics and Engineering*, 196(7):1216–1243, 2007.
- [5] Jean-Claude Michel and Pierre Suquet. Nonuniform transformation field analysis. *International journal of solids and structures*, 40(25):6937–6955, 2003.
- [6] SP Triantafyllou and EN Chatzi. A hysteretic multiscale formulation for nonlinear dynamic analysis of composite materials. *Computational Mechanics*, 54(3):763–787, 2014.
- [7] Dongbin Xiu and George Em Karniadakis. The wiener–askey polynomial chaos for stochastic differential equations. *SIAM journal on scientific computing*, 24(2):619–644, 2002.
- [8] M Jardak and RG Ghanem. Spectral stochastic homogenization of divergence-type pdes. *Computer Methods in Applied Mechanics and Engineering*, 193(6):429–447, 2004.
- [9] Stefano Marelli and Bruno Sudret. Uqlab: a framework for uncertainty quantification in matlab. In *Vulnerability, Uncertainty, and Risk: Quantification, Mitigation, and Management*, pages 2554–2563. 2014.
- [10] Norbert Wiener. The homogeneous chaos. *American Journal of Mathematics*, 60(4):897–936, 1938.
- [11] Robert H Cameron and William T Martin. The orthogonal development of non-linear functionals in series of fourier-hermite functionals. *Annals of Mathematics*, pages 385–392, 1947.
- [12] Bradley Efron, Trevor Hastie, Iain Johnstone, Robert Tibshirani, et al. Least angle regression. *The Annals of statistics*, 32(2):407–499, 2004.
- [13] Géraud Blatman and Bruno Sudret. Adaptive sparse polynomial chaos expansion based on least angle regression. *Journal of Computational Physics*, 230(6):2345–2367, 2011.
- [14] Minas D Spiridonakos, Eleni N Chatzi, and Bruno Sudret. Polynomial chaos expansion models for the monitoring of structures under operational variability. *ASCE-ASME Journal of Risk and Uncertainty in Engineering Systems, Part A: Civil Engineering*, 2(3):B4016003, 2016.

- [15] Yunus E Harmanci, Minas D Spiridonakos, Eleni N Chatzi, and Wolfram Kübler. An autonomous strain-based structural monitoring framework for life-cycle analysis of a novel structure. *Frontiers in Built Environment*, 2:13, 2016.
- [16] Jerome Friedman, Trevor Hastie, and Robert Tibshirani. *The elements of statistical learning*, volume 1. Springer series in statistics Springer, Berlin, 2001.
- [17] Bruno Sudret. Global sensitivity analysis using polynomial chaos expansions. *Reliability Engineering & System Safety*, 93(7):964–979, 2008.